Supplementary Information

Phagolysosome resolution requires contacts with the ER and phosphatidylinositol 4-phosphate signaling

Roni Levin-Konigsberg[1,2,3], Fernando Montaño-Rendón [1,4], Tal Keren-Kaplan[5], Ren Li[1], Braeden Ego[3], Sivakami Mylvaganam[1,2] Jessica E. DiCiccio[1,2], William S. Trimble[1,2], Michael C. Bassik[3], Juan S. Bonifacino[5], Gregory D. Fairn*[2,6] and Sergio Grinstein*[1,,2,4,6]

1. Division of Cell Biology, Hospital for Sick Children, Toronto, Ontario, Canada
2. Department of Biochemistry, University of Toronto, Toronto, Ontario, Canada
3. Department of Genetics, Stanford University School of Medicine, Stanford, CA, USA
4. Institute of Medical Sciences, University of Toronto, Toronto, Ontario, Canada
5. Cell Biology and Neurobiology Branch, Eunice Kennedy Shriver National Institute of Child Health and Human Development, National Institutes of Health, Bethesda, MD, USA
6. Keenan Research Centre for Biomedical Science, St. Michael's Hospital, Toronto, Ontario, Canada

* Address correspondence to sergio.grinstein@sickkids.ca and FairnG@smh.ca

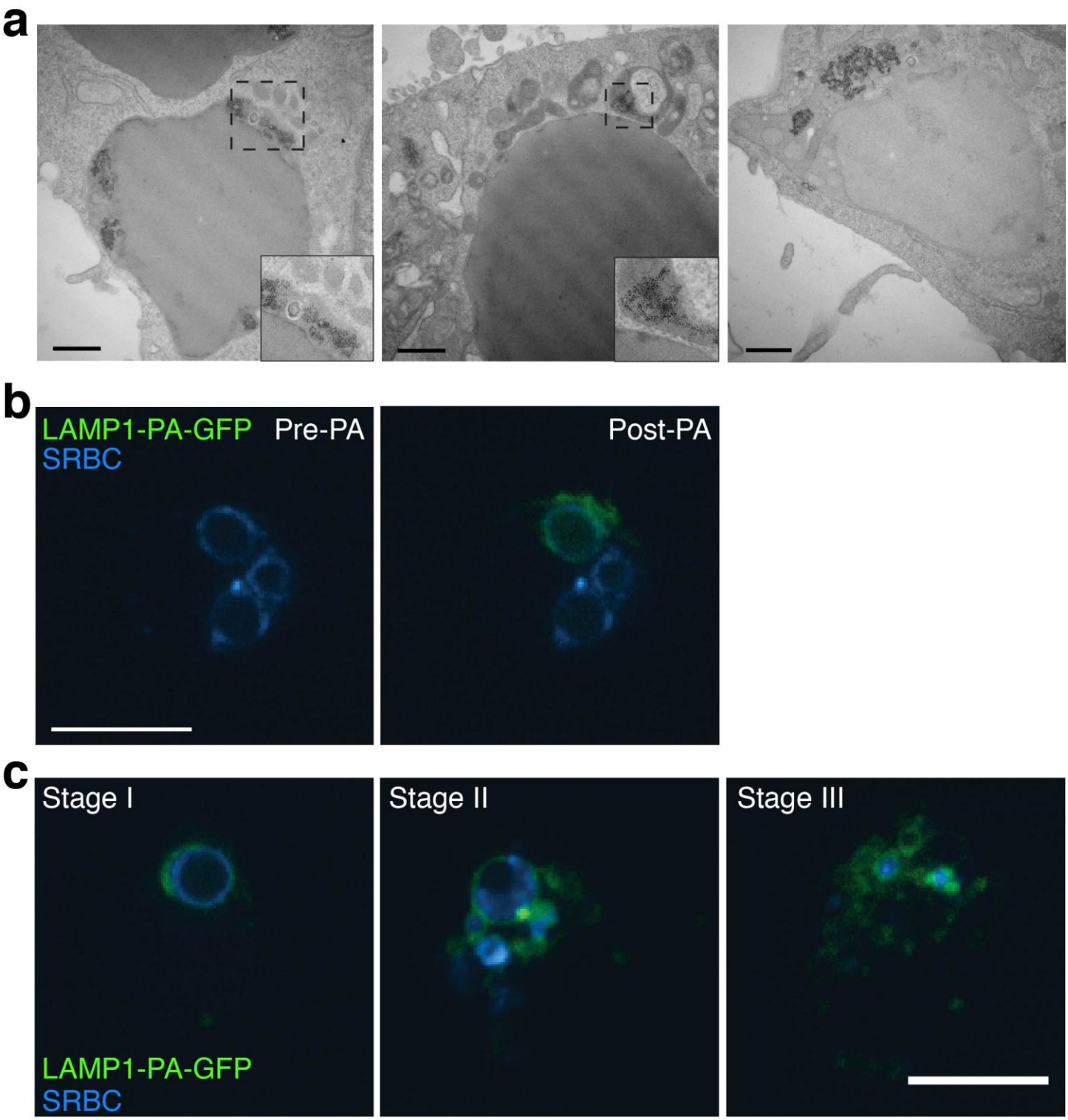

Supplementary Figure 1

Dispersed compartments during phagosome resolution are of phagosomal origin

a) Transmission electron micrographs of RAW macrophages during stage II of phagosome resolution of IgG-

SRBC pre-labeled with ferritin; experiment was repeated independently 3 times with similar observations; scale bars = 1 µm b) Confocal micrograph of RAW macrophages after 30 min of phagocytosis of IgG-SRBC (blue); cells were expressing LAMP1-PAGFP; micrographs were acquired before (left) and after activation of LAMP1-PAGFP in the membrane of an individual phagosome (right); similar observations were made in 5 independent experimental replicates. c) Time-lapse micrographs of RAW macrophages expressing LAMP1-PAGFP during the three stages of phagosome resolution; the phagosomal membrane was photo-activated after 30 min of phagocytosis; similar results were observed in 3 independent experiments; scale bars in b-c = 10 µm.

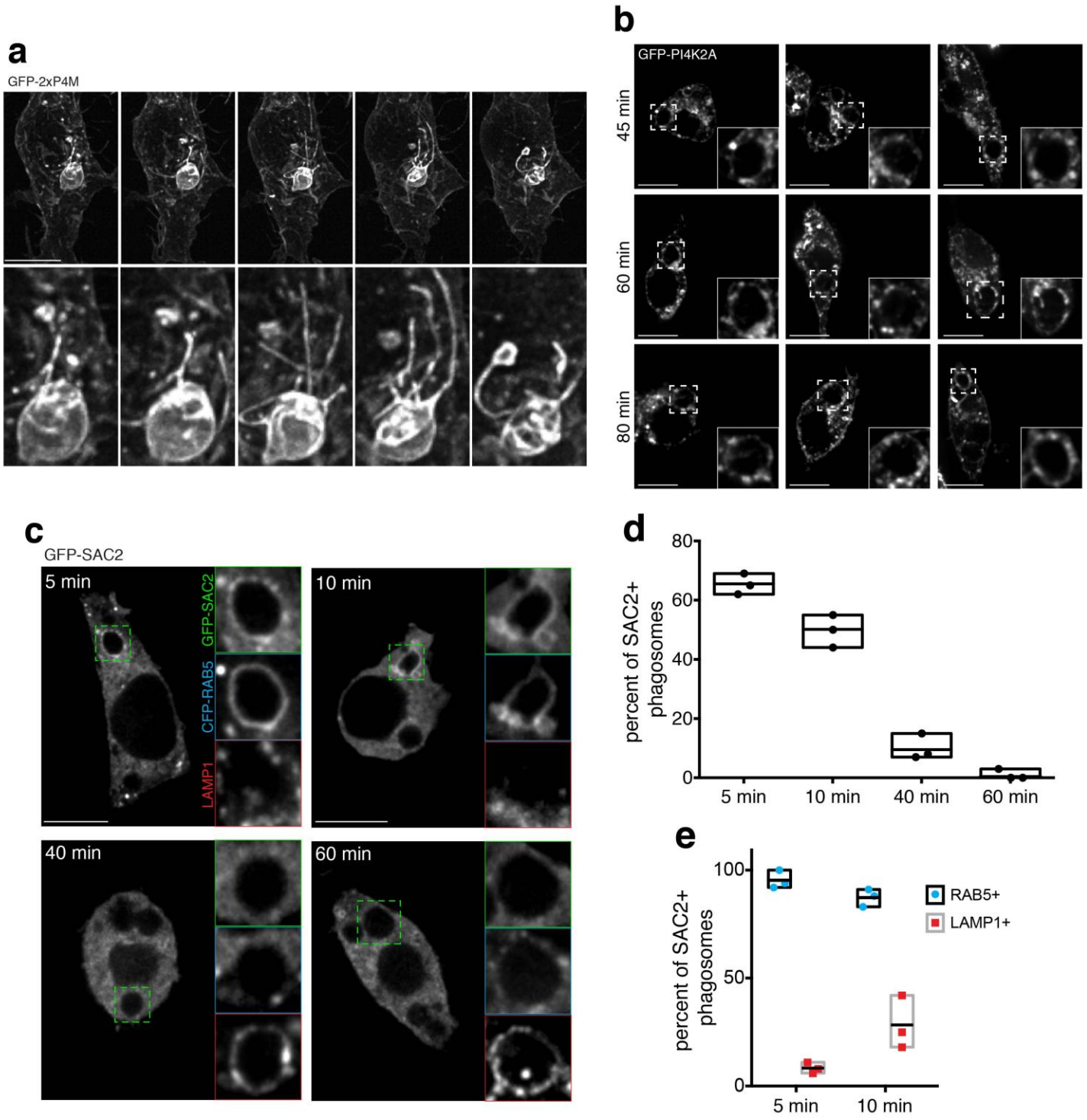

Supplementary Figure 2

PtdIns4P dynamics and metabolism during the transition from phagolysosome biogenesis to phagosome resolution

a) Time-course gallery of maximum intensity projections of lattice light-sheet micrographs of RAW macrophages expressing GFP-2xP4M during late stages of phagocytosis of SRBC; similar observations were

made in 2 independent experimental repeats. b) Representative confocal micrographs of RAW cells expressing GFP-PI4K2A during the transition from late phagosome maturation to early phagosome resolution at 45, 60 and 80 min of phagocytosis; similar results were obtained from 10 independent experimental replicates. c) Time-course gallery of representative confocal micrographs of RAW macrophages co-expressing GFP-SAC2 and CFP-RAB5, and immunostained with an anti-LAMP1 antibody. The main micrographs show GFP-SAC2; insets show magnifications of phagosomes in dashed boxes; similar results were observed in 3 independent replicates; scale bars = 10 µm. d) Means and individual values of 3 independent replicate determinations of the percentage of SAC2-positive phagosomes at the indicated times of phagocytosis. e) Means and individual values of 3 independent replicate determinations of the percentage of SAC2-positive phagosomes that are also positive for RAB5 (blue circles) or LAMP1 (red squares).

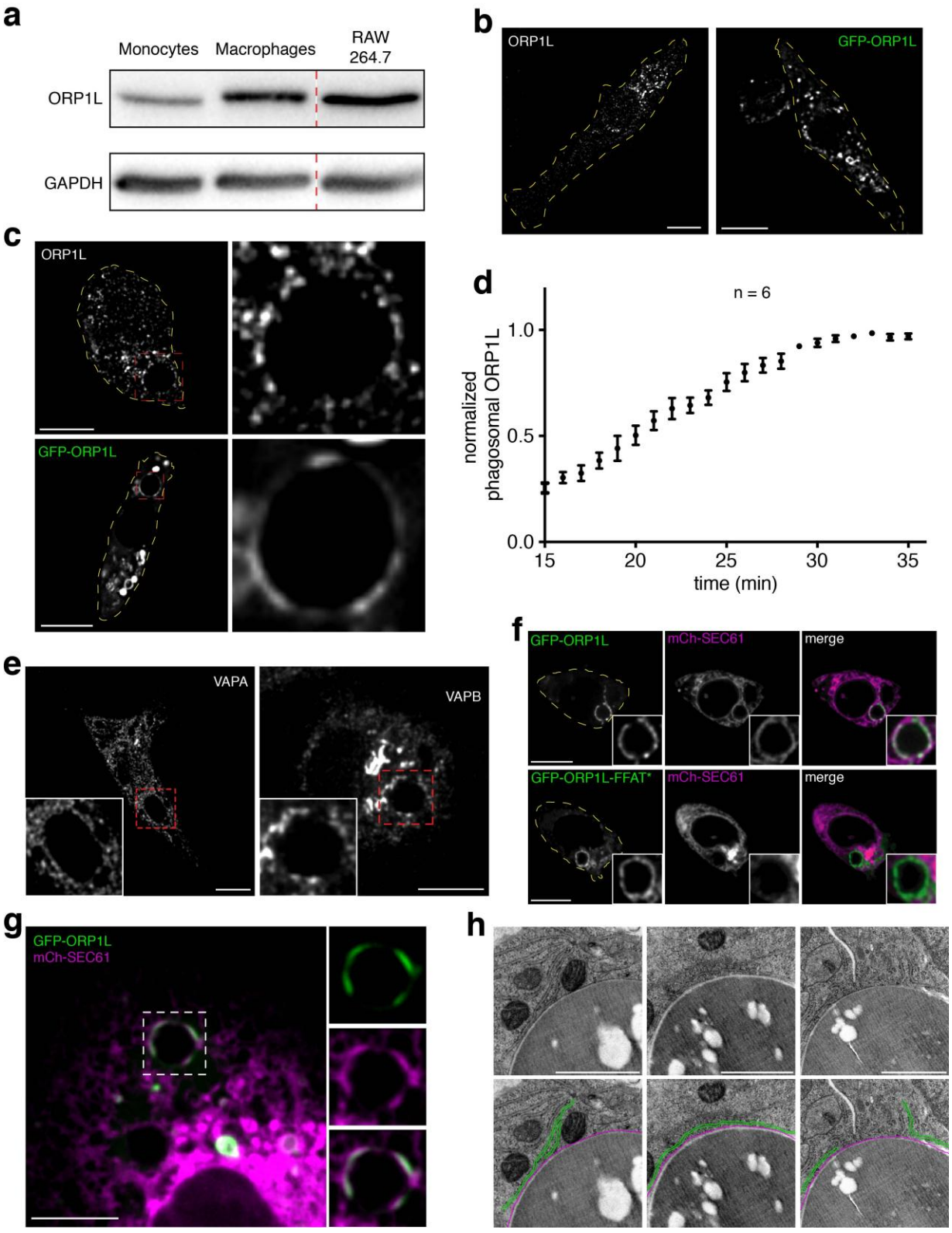

Supplementary Figure 3

ORP1L localizes to phagosomes and mediates contacts with the ER

a) Representative immunoblot showing ORP1L expression in primary human monocytes and macrophages, and in murine RAW macrophages; similar results were obtained from 2 independent replicates. b) Endomembrane localization of endogenous ORP1L in primary human macrophages (left) and of GFP-ORP1L expressed in RAW macrophages (right); similar observations were made in 3 independent experimental replicates. c) *Top*: endogenous localization of ORP1L in primary human macrophages during phagocytosis of IgG-opsonized RBC; yellow lines show the cell periphery; magnification of phagosome within red box (right). *Bottom*: localization of ectopically expressed GFP-ORP1L during phagocytosis; other details as above; similar observations were made in 3 independent replicates. d) Kinetics of accumulation of ORP1L in maturing phagosomes of RAW macrophages; means of 6 experimental replicates ± SEM. e) Immunolocalization of endogenous VAPA (*left*) or VAPB (*right*) in primary human macrophages after 40 min of phagocytosis of RBC; insets show magnification of the phagosome in the red box; representative of 3 independent replicate experiments. f) Confocal micrographs showing RAW macrophages co-expressing GFP-ORP1L and mCh-SEC61 (*top)*, or GFP-ORP1L-FFAT* and mCh-SEC61 (*bottom)*; representative of 5 independent experimental replicates. g) Confocal micrographs showing COS-2A cells co-expressing GFP-ORP1L and mCh-Sec61; representative results of 3 independent experiments. h) Transmission electron micrographs of RAW macrophages after 40 min of phagocytosis showing close appositions between the ER and phagosomal membranes. Bottom panels highlights ER membranes (colored in green) that are in contact with the phagosomal membrane (colored in magenta); similar observations were made in 3 independent experimental replicates. Scale bars = 10 µm except for *h*, where scale bars = 1 µm.

Figure S4

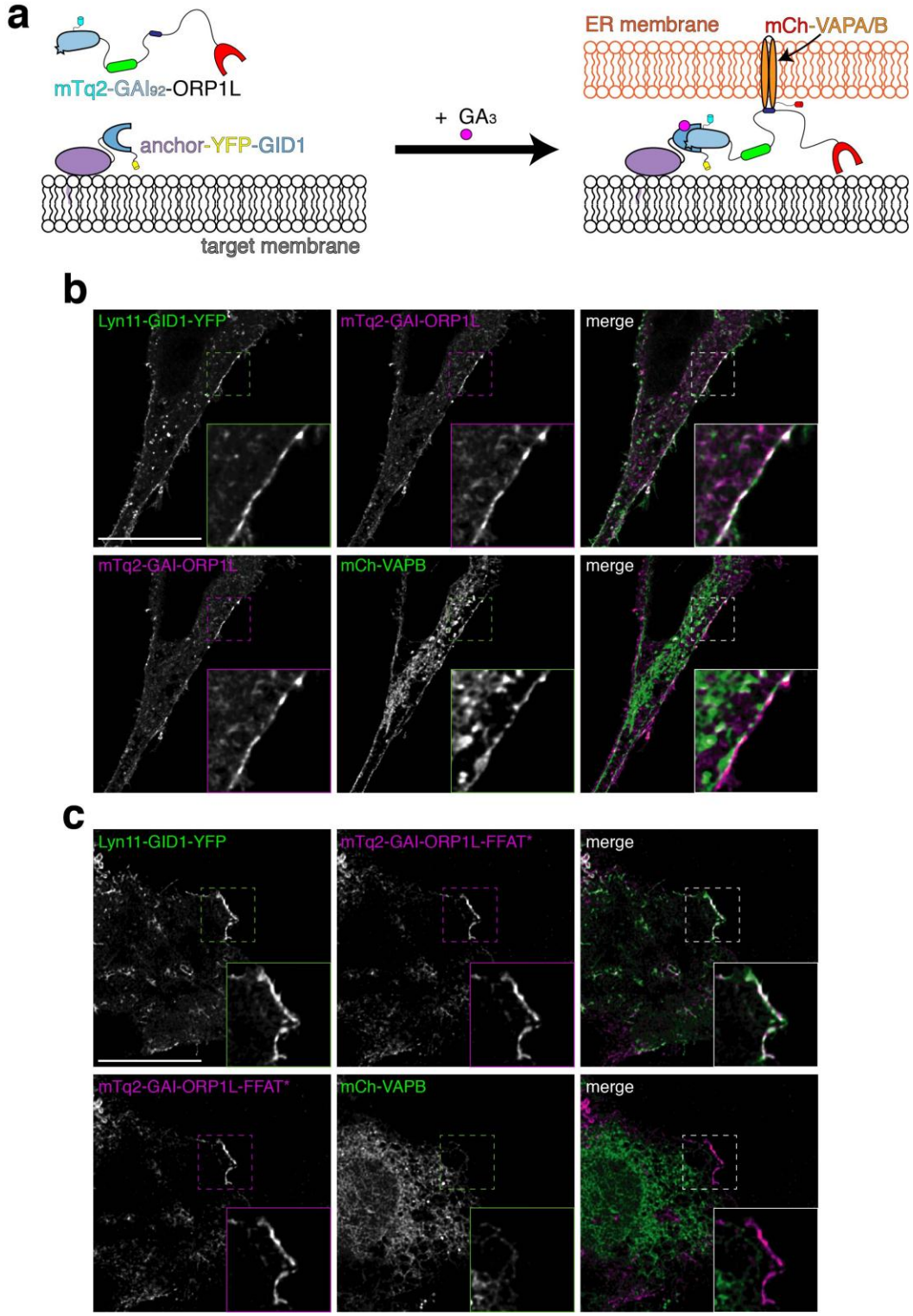

Supplementary Figure 4

ORP1L mediates ER contact sites through its FFAT motif

a) Schematic representation of the gibberellin-induced dimerization system. ORP1L variants (WT and FFAT*) lacking ankyrin repeats were rendered soluble ($ORP1L_{747}$). These variants were linked to the smallest recruitable fragment of the gibberellin insensitive protein GAI (GAI_{92})[46] and tagged with mTurquoise2. A second construct consists of YFP-tagged gibberellin-insensitive dwarf1 (GID1) linked to the 11 amino acid tail of Lyn kinase that localizes to the plasma membrane. The plant hormone gibberellin binds GID1 causing a conformational change. The alternative GID1 conformation recruits the gibberellin-insensitive protein GAI. After addition of a cell permeant gibberellin analog (GA_3-AM), the soluble mTq2-GAI_{92}-$ORP1L_{747}$ is recruited to the PM. b-c) Representative confocal micrographs of 3 independent experimental replicates showing HeLa cells expressing mCh-VAPB, YFP-GID1-Lyn11 and either mTq2-GAI_{92}-$ORP1L_{747}$ (b) or its FFAT* variant (c), after the addition of GA_3-AM.

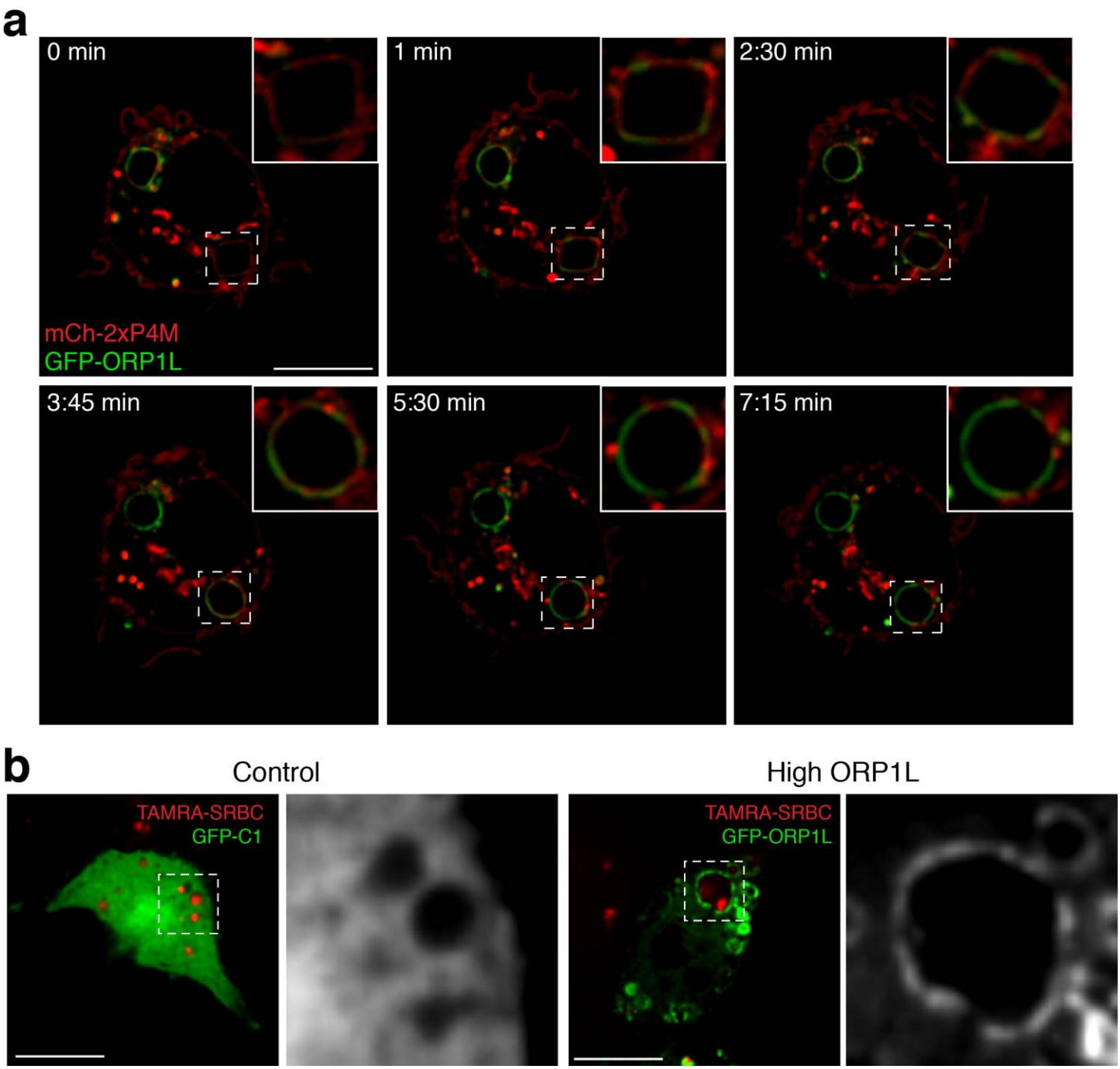

Supplementary Figure 5

PtdIns4P and ORP1L localize to mutually exclusive phagosomal microdomains

a) Representative time-lapse gallery of confocal micrographs showing mutual exclusion between PtdIns4P (detected with mCh-2xP4M) and GFP-ORP1L. b) Confocal slice of RAW macrophages expressing either soluble GFP (*left*) or GFP-ORP1L (*right*) after 4.5 h of phagocytosis of TAMRA-labeled RBC; insets show magnifications of the green channel of the dotted white boxes. Scale bars = 10 µm.

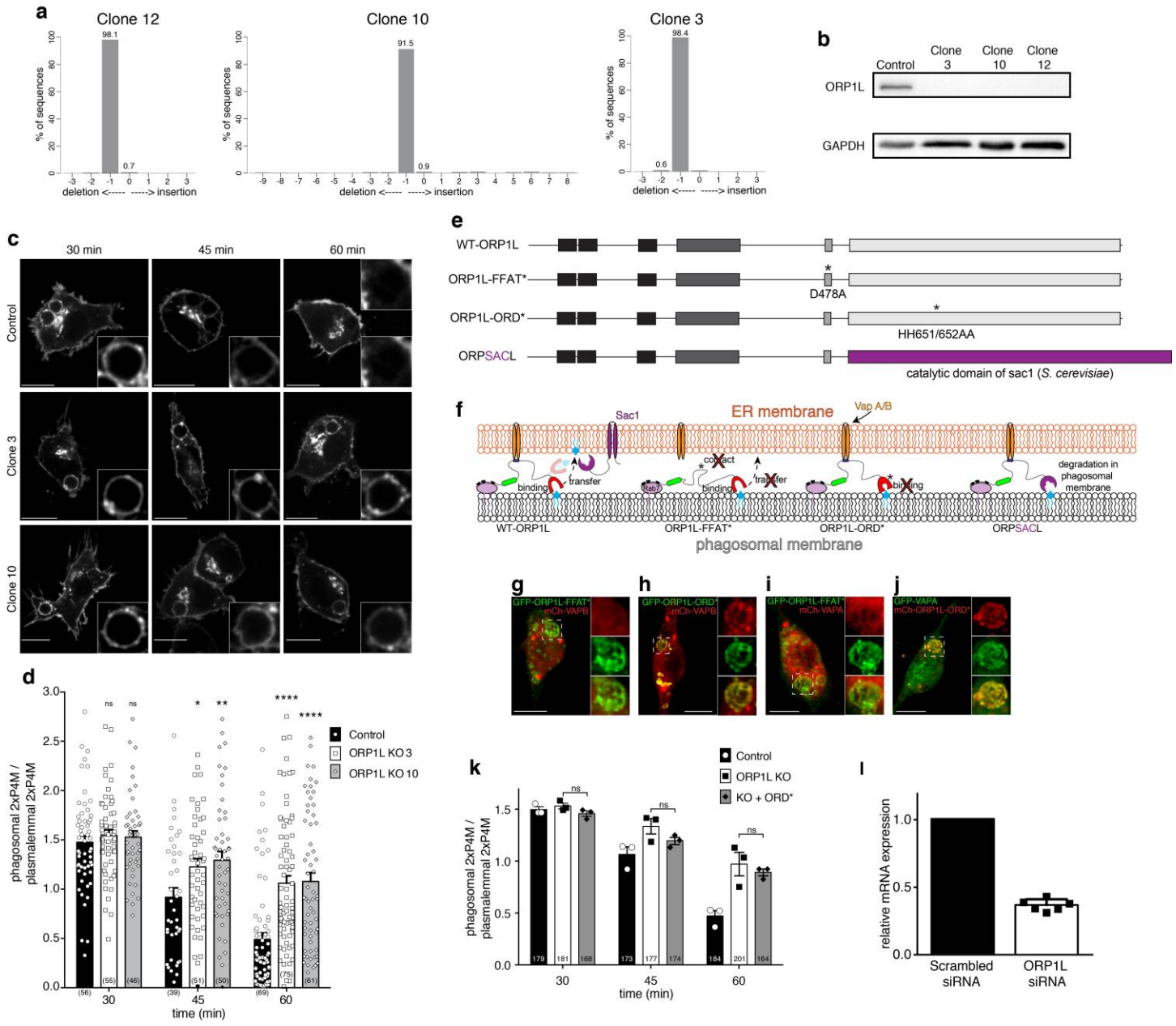

Supplementary Figure 6

Impairment of PtdIns4P disappearance by ORP1L KO clones and ORP1L variants.

a) TIDE analysis of a homozygous ORP1L CRISPR KO clonal RAW macrophage cell lines. b) Representative western blot showing expression of ORP1L in WT, control (cells stably expressing Cas9 and transduced with control sgRNA) and ORP1L KO RAW macrophage cell lines. c) Representative confocal micrographs of 3 independent replicates showing control or ORP1L KO RAW macrophages expressing GFP-2xP4M at the indicated times during phagosome maturation. Scale bars = 10 µm. d) PtdIns4P dynamics in maturing phagosomes of control cells (black bars), ORP1L KO clone "3" (white bars) and ORP1L KO clone "10"

(stippled bars); means of ≥ 39 phagosomes per time-point and per condition, from 3 experimental replicates ± SD; significance was determined by two-way ANOVA using Sidak correction, details are in the statistics source data supplementary file. e) Schematic representation of: (from top to bottom) WT ORP1L; ORP1L with a mutated FFAT motif (D478A) incapable of binding VAPA/B; ORP1L with a mutated lipid-binding pocket within the ORD (HH651/652AA) predicted to abolish PtdIns4P binding; ORPSAC1, in which the ORD was replaced with the phosphatase domain of Sac1 from *S. cerevisiae*. f) Schematic representation of the predicted behavior of each ORP1L variant at ER-phagosome contacts. g-j) Representative maximum intensity projections of three independent replicates of RAW cells after 30 min of phagocytosis of SRBC expressing: g) GFP-ORP1L-FFAT* and mCh-VAPB; h) mCh-ORP1L-ORD* and GFP-VAPB; i) GFP-ORP1L-FFAT* and mCh-VAPA; and j) GFP-ORP1L-ORD* and mCh-VAPA. Insets show magnifications of each channel and merged image at bottom. Scale bars = 10 µm. k) Phagosomal 2xP4M (normalized to PM) in control cells, ORP1L KO cells (replotted from Fig. 5b) and for ORP1L KO cells expressing GFP-ORP1L-ORD*. Data are means ± SD of the indicated number of determinations from 3 independent experiments. Significance calculated using two-way ANOVA with Sidak correction, assuming statistical independence between groups, details are in the statistics source data supplementary file. l) Relative mRNA levels of control RAW cells treated with scrambled siRNA cells (black bar) or treated with siRNA against *Orp1l*, measured by qPCR; means ± SD of six independent experiments normalized individually to mRNA levels of paired cells treated with scrambled siRNA.

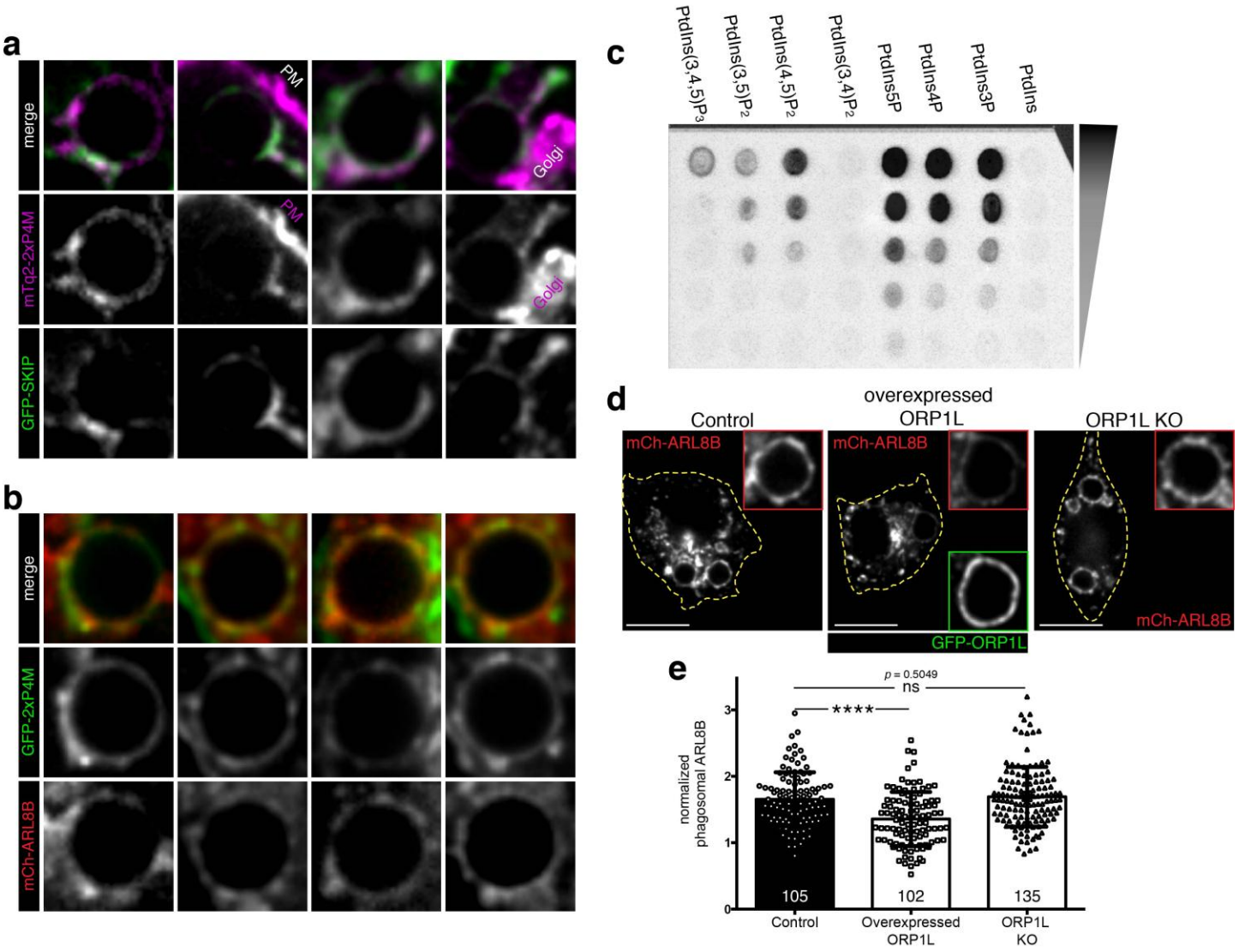

Supplementary Figure 7

PtdIns4P implications with the association of SKIP – ARL8B to the phagosomal membrane

a-b) Representative confocal micrographs of 3 independent experimental replicates showing phagosomes in RAW macrophages transfected with (a) GFP-SKIP and mTq2-2xP4M or (b) mCh-ARL8B and GFP-2xP4M. c) Protein overlay assay; a hydrophobic membrane spotted with the indicated lipids and overlaid with purified recombinant GST-SKIP (0.6 µg/mL); bound protein was detected by immunoblotting; similar results were observed in 3 independent replicates. d) Representative confocal micrographs of 3 independent experimental replicates showing RAW macrophages expressing mCh-ARL8B after 45 min of phagocytosis of IgG-SRBC under: control conditions (left panel); overexpression of mCh-ORP1L (middle panel); and ORP1L KO (right panel). e) Quantitation of ARL8B recruitment to phagosomes under the conditions shown in f. Means ± SEM of the number of determinations indicated in each bar, from 3 independent experiments. Significance determined by two-tailed unpaired *t* tests; ****$p \leq 0.0001$.

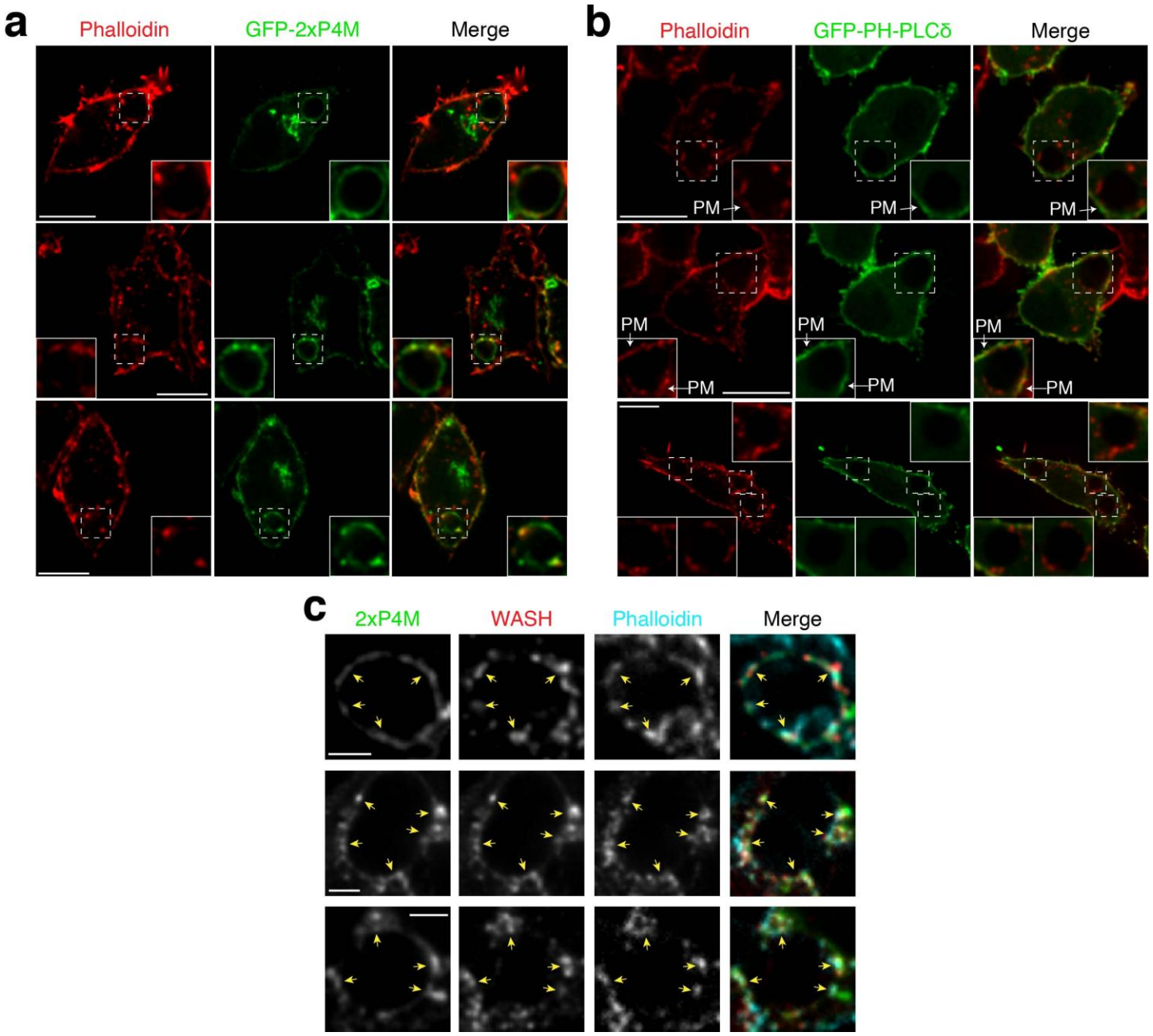

Supplementary Figure 8

PtdIns4P-positive phagosomal membrane domains are enriched in actin and WASH and do not contain PtdIns(4,5)P_2

a) Representative confocal micrographs of 3 independent replicate experiments showing RAW macrophages expressing GFP-2xP4M, fixed after 45 min of phagocytosis and stained with phalloidin conjugated to Alexa Fluor 568. Each row shows different cells under the same conditions. b) Representative confocal micrographs of 3 independent replicate experiments showing RAW macrophages expressing GFP-PH-PLCδ, fixed after 45 min of phagocytosis and stained with phalloidin conjugated to Alexa Fluor 568. Insets are magnifications of

individual phagosomes. Scale bars in (a) and (b) = 10 µm. c) Representative confocal micrographs of 3 independent replicate experiments showing of phagosomes of RAW macrophages expressing GFP-2xP4M that were fixed and immunostained for endogenous WASH and labeled with phalloidin 45 min after phagocytosis. Scale bars = 2.5 µm.

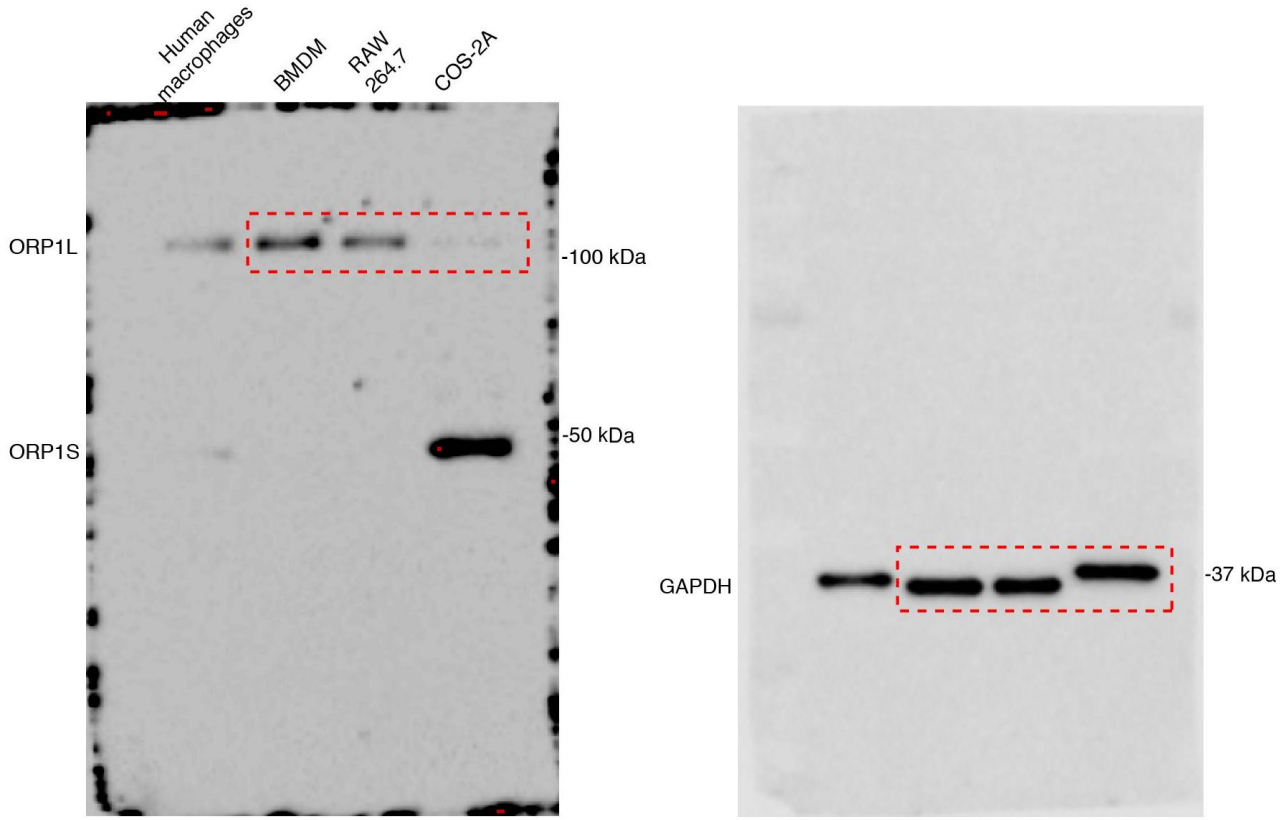

Supplementary Figure 9

Unprocessed images of all gels and blots

Unprocessed western blot from Fig. 6a

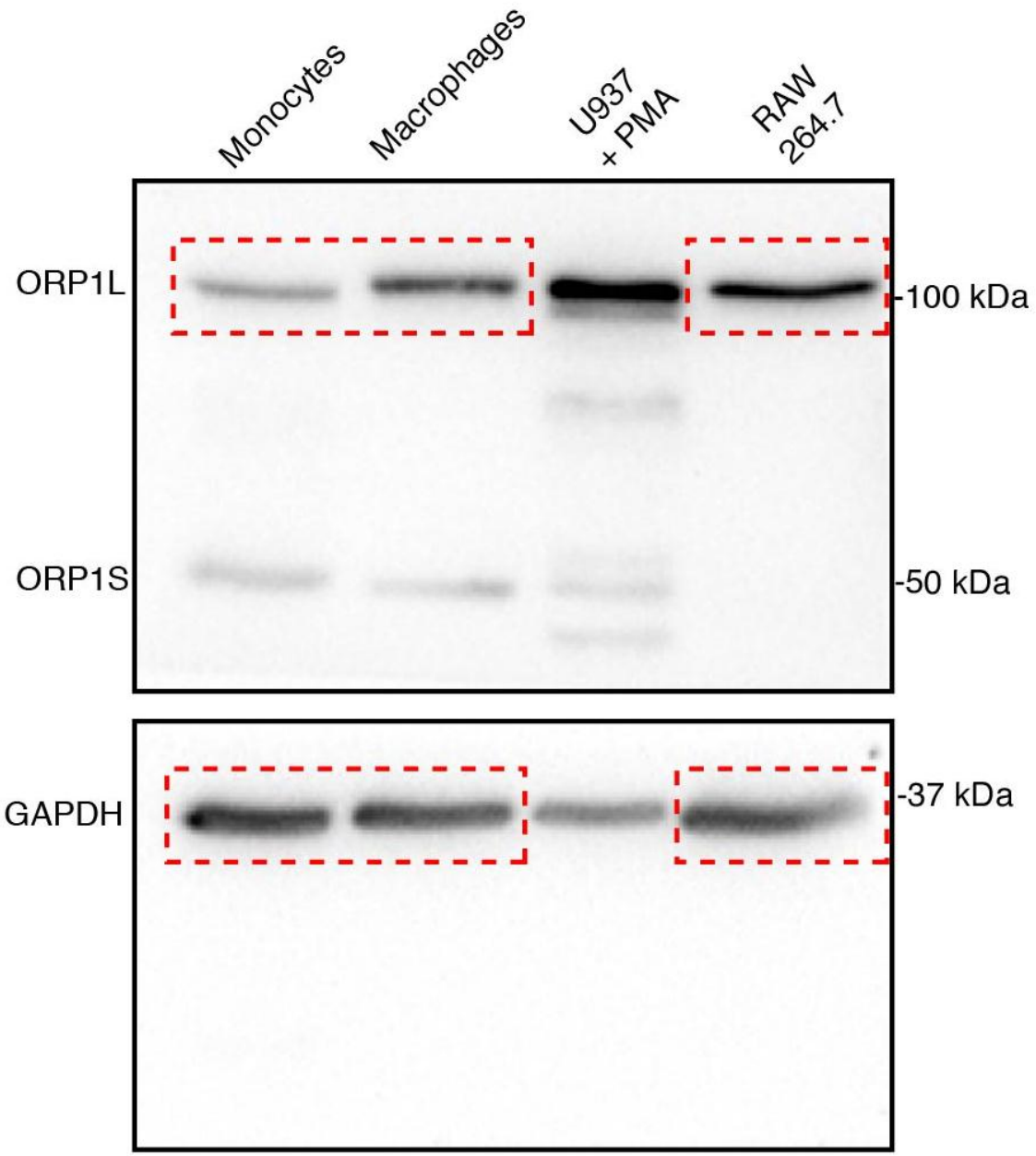

Supplementary Figure 9

Unprocessed images of all gels and blots (continued)

Unprocessed western blot from Fig. S3a

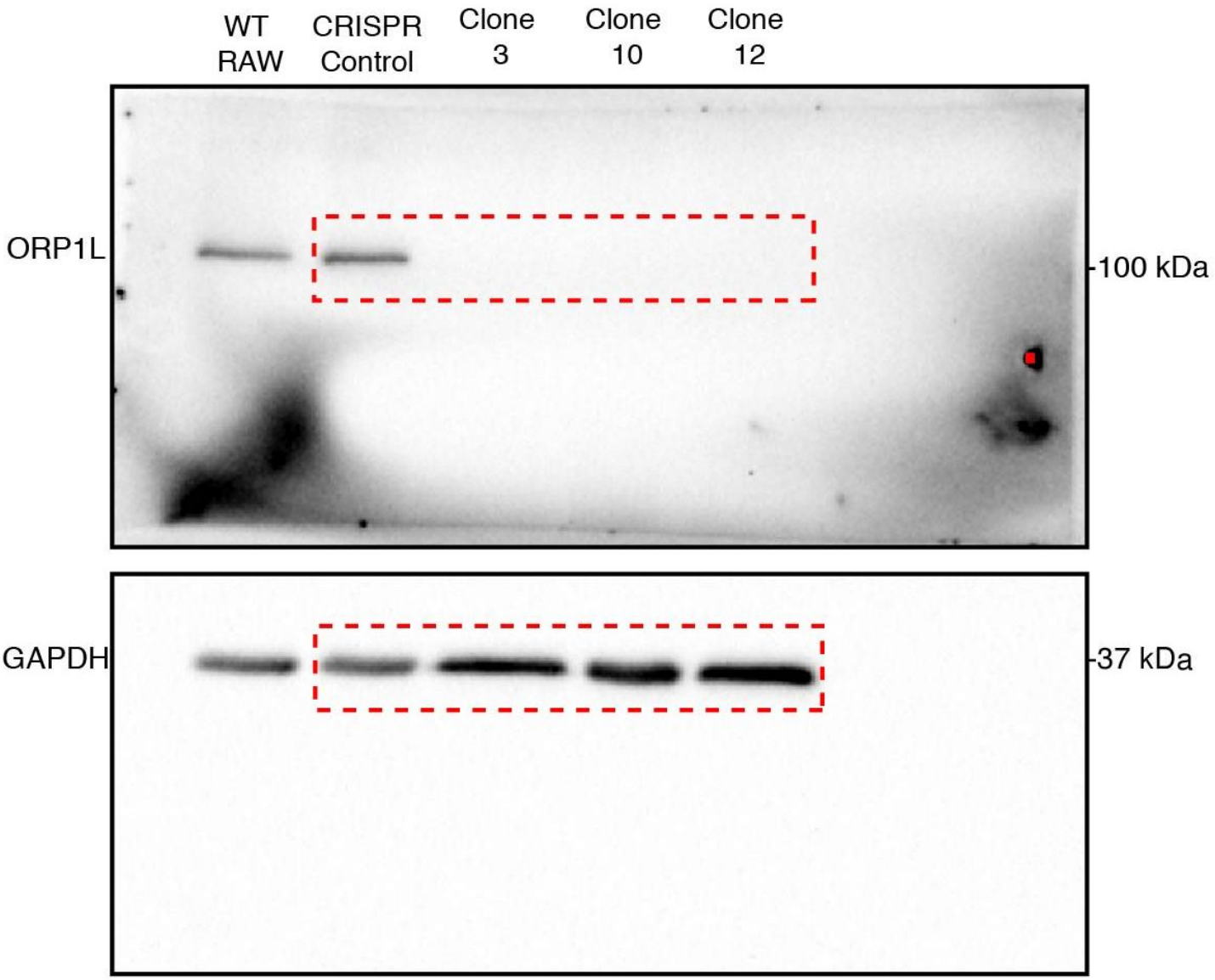

Supplementary Figure 9

Unprocessed images of all gels and blots (continued)

Unprocessed western blot from Fig. S6B

Supplementary Table 1

Plasmids

List of plasmids used in this study

Supplementary Table 2

Statistics Source Data

Source data for quantifications and statistic results are provided

REFERENCES

1. Harrison, R. E., Bucci, C., Vieira, O. V., Schroer, T. A. & Grinstein, S. Phagosomes fuse with late endosomes and/or lysosomes by extension of membrane protrusions along microtubules: role of Rab7 and RILP. *Mol. Cell. Biol.* **23,** 6494–6506 (2003).
2. Weir, M. L., Xie, H., Klip, A. & Trimble, W. S. VAP-A binds promiscuously to both v- and tSNAREs. *Biochem. Biophys. Res. Commun.* **286,** 616–621 (2001).
3. Johnson, D. E., Ostrowski, P., Jaumouillé, V. & Grinstein, S. The position of lysosomes within the cell determines their luminal pH. *J. Cell Biol.* **212,** 677–692 (2016).